Available online at www.sciencedirect.com
SCIENCE DIRECT
Polymer 46 (2005) 9155–9161
polymer
www.elsevier.com/locate/polymer

A molecular simulation study of cavity size distributions and diffusion in *para* and *meta* isomers

Xiao-Yan Wang, Pieter J. in 't Veld[1], Ying Lu, Benny D. Freeman, Isaac C. Sanchez*

Department of Chemical Engineering, University of Texas at Austin, Austin, TX 78712, USA

Received 27 May 2005; received in revised form 28 June 2005; accepted 29 June 2005
Available online 9 August 2005

Abstract

Polysulfone based on bisphenol A has been extensively used as a material for membrane-based gas separation. For polymers with aromatic rings in their backbones, such as polysulfones and polyimides, changing the connecting bond positions from *meta* to *para* seems to increase their permeability and diffusivity to gases. Cavity size distributions of three isomer pairs (PSF and 3,4′-PSF, PSF-P and PSF-M, 6FDA-6F*p*DA and 6FDA-6F*m*DA) are calculated through molecular simulation. The diffusivity of small molecules in these isomers is also obtained by molecular dynamics. For all three isomer pairs, the average cavity size in *para* isomers is larger than in *meta* isomers. The molecular dynamics determined diffusion coefficients of neon in *para* isomers are also larger than in *meta* isomers. These results are consistent with the experimental observation that room-temperature gas diffusion in *para* isomers is faster than in *meta* isomers.

Keywords: Molecular simulation; Cavity size distribution; Free volume

1. Introduction

Polymer membranes have a wide industrial application in gas separation. Polysulfone based on bisphenol A has been extensively used as a material for membrane-based gas separation [1–4]. Fluorine-containing polyimides are also interesting polymers for application as membranes because of their excellent thermal, mechanical, and gas transport properties [5–9].

Several studies have revealed the interesting effects of structural symmetry on gas transport properties of a number of polymers such as polysulfones [3,4], polyimides [5–9], polyester [10], poly(phenolphthalein phthalates) [11], and poly(methyl methacrylate) [12] and polycarbonates [13]. For polymers with aromatic rings in their backbones, such as polysulfones and polyimides, changing the connecting bond positions from *meta* to *para* increases their permeability and diffusivity to gases [4,8,9]. This is somewhat surprising because the glass temperature of the *para* isomer is always greater than the *meta* isomer [11]. Coleman and Koros, in their study of polyimides [8,9], have observed relatively large decreases in permeability and large increases in permselectivity when *para* linkages are replaced with *meta* linkages. It was proposed that a restriction in the sub-T_g motions of the unsymmetric polyimides may account for these changes. The interesting symmetrical effects seem to provide a means to improve the separation properties of membranes materials, so a fundamental investigation of these effects will aid in new membrane material design.

Molecular modeling techniques have been widely used to obtain better theoretical understanding of the relationship between chemical structure, including effect of the symmetry, and the transport behavior of non-porous amorphous polymer membranes [14–29]. Pavel and Shanks [14] have simulated the diffusion of oxygen and carbon dioxide in amorphous poly(ethylene terephthalate) and showed that the diffusion coefficients for both oxygen and carbon dioxide molecules increased exponentially with an increase in free volume. It was also found that the *ortho*, *meta* and *para* isomers of the aromatic moiety have a significant influence on the diffusion coefficient. The diffusion coefficients for both oxygen and carbon dioxide

* Corresponding author. Tel.: +1 512 471 1020.
E-mail address: sanchez@che.utexas.edu (I.C. Sanchez).
[1] Current Address: Sandia National Laboratories, MS 1415, Albuquerque, NM 87185-1415, USA.

0032-3861/$ - see front matter © 2005 Elsevier Ltd. All rights reserved.
doi:10.1016/j.polymer.2005.06.122

molecules in all of the simulated polyesters decrease from *para* to *ortho* and *meta* like isomers.

Transition-state theory (TST) is an alternative method to predict the diffusion coefficients and the solubility values [15,16,19–21,24,26]. Karayiannis and his co-workers [16] have calculated diffusion coefficients of oxygen molecules in two polyisomers, poly(ethylene terephthalate) (PET) and poly(ethylene isophthalate) (PEI) by employing TST technique. Calculated O_2 diffusivities are in good agreement with experiments: O_2 diffusivity in PET (*para*) is predicted 1.8 times larger than in PEI (*meta*), in agreement with experimental finding that PET is 2–2.5 times more permeable to O_2 than PEI.

A diffusion theory for simple liquids, which connects small molecule diffusion to the minimum cavity size needed for the diffusant and the system's mean free volume, was developed by Cohen and Turnbull [30]. Thran et al. [31] have published a review of this approach for polymers. The total free volume is undoubtedly the dominant factor for diffusion as well as permeation. Cavity size distribution [32,33] gives a detailed description of how the free volume elements are distributed over the system. The extent to which the distribution of free volume affects diffusion is also important, especially for systems that have comparable total free volume, but very different permeabilities [34–36].

Very recently, our group has developed a new algorithm [32], the cavity energetic sizing algorithm (CESA), for determining the cavity size distribution in liquids. CESA is based on energetic rather than geometric considerations for cavity definition and is applicable to any structure that can be simulated by molecular dynamic or Monte Carlo methods. CESA was verified by application to crystalline structures with well-characterized cavities. It has also been applied to hard sphere and Lennard–Jones fluids, SPC/E water, as well as to two very permeable polymers, poly(1-trimethylsilyl-1-propyne) (PTMSP) and a random copolymer of tetrafluoroethylene and 2,2-bis(trifluoromethyl)-4,5-difluoro-1,3-dioxole (TFE/BDD) [32,35,36]. Delaunay and Voronoi tessellation, a geometrical approach to describe cavity size distribution, has also been employed to characterize glassy polymers [34]. Schmidtke et al. [37] presented an improved method to describe the unoccupied volume in glassy polymers, and they also applied the method to determine the unoccupied volume of molecular dynamic simulations of poly(amide imide) unit cells by probing it using a tracer atom. Since this method uses a tracer atom, the reachable unoccupied volume strongly depends on the tracer radius.

Cavity size (free volume) distribution can also be measured experimentally on the atomic scale using positron annihilation lifetime spectroscopy (PALS). In PALS, the pick-off lifetime of the $^3S_1$ state of positron (a hydrogen-like *ortho*-positronium atom, *o*-Ps) was used to measure hole sizes in the polymers. PALS has been applied to measure free-volume size distribution in various polymer samples [38–42]. The average cavity sizes for PTMSP and TFE/BDD calculated using CESA are consistent with PALS measurements [35,36,42].

This paper presents cavity size distributions determined by CESA for one pair of polyimide isomers and two pairs of polysulfone isomers. The structure and physical properties of three pairs are presented in Tables 1 and 2. Notice that the *meta* isomers have lower fractional free volumes, lower glass transition temperatures, lower diffusivity and permeability than the *para* isomers. The diffusivity of neon in these isomers is also obtained by molecular dynamics.

2. Simulation

Molecular dynamics (MD) simulation was performed using the Amorphous Cell module of Materials Studio and Cerius2 packages [43] to obtain polymer structures. The COMPASS [44] (condensed-phase optimized molecular potentials for atomistic simulation studies) forcefield was applied to model all three *para* and *meta* isomer pairs in an atomistic way. The non-bonded interactions of COMPASS force field include a Lennard–Jones 9-6 function for the van der Waals (VDW) term and a coulombic function for the electrostatic interaction. Each isomer chain was built from 20 repeat units. The initial states were generated at the experimental densities (which are listed in Table 2) for all isomers. The length of the cubic unit cell was 18–26 Å. Some simulation data are listed in Table 3. Fifty initial states were constructed for each polymer and followed by 5000 steps of energy minimization to 'melt' the high energy spots. Afterwards, a 60 ps NVT MD run was performed for each of the 50 states to equilibrate. Fifty initial states for each isomer represent 50 isomer samples. Cavity size distribution, average cavity size and fractional cavity volume (FCV) properties were an average over 50 samples. Polysulfones and polyimides are very stiff polymers, and it is not easy to obtain uncorrelated structures from just one initial state. Therefore we generated 50 initial states in order to get 50 uncorrelated structures. Most other simulation work [14–16,22] use 1–5 samples with each sample going through longer simulation times. We are confident in this 'many initial states' strategy based on our previous simulation work with PTMSP and TFE/BDD. The cavity size distributions and average cavity sizes of these two polymers we simulated are in good agreement with PALS data. The simulated permeability, diffusivity and solubility are also in good agreement with experimental data [35,36].

The cavity energetic sizing algorithm (CESA) was then applied to the equilibrated structures of each polymer to obtain cavity size distribution, average cavity size and FCV. The details of CESA were given in our previous paper [32]. The following is a brief summary of the CESA method.

(i) A polymer structure is generated by MD (or MC) simulation.

Table 1
Structures of *para* and *meta* isomers studied [4,8]

Polymer	Structure
PSF	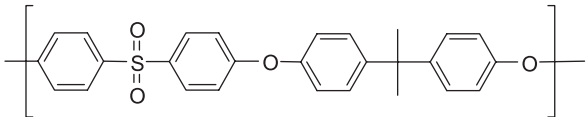
3,4′-PSF	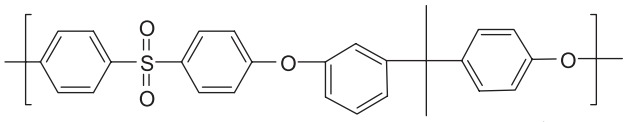
PSF-P	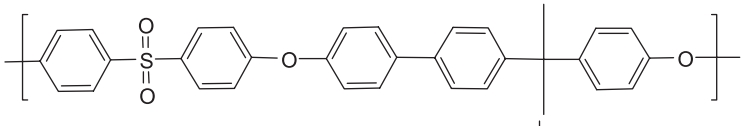
PSF-M	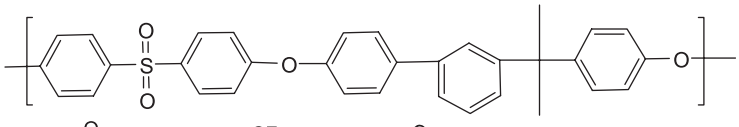
6FDA-6F*p*DA	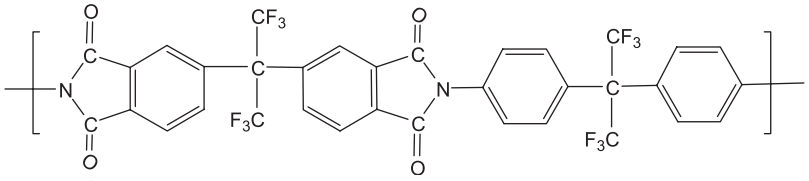
6FDA-6F*m*DA	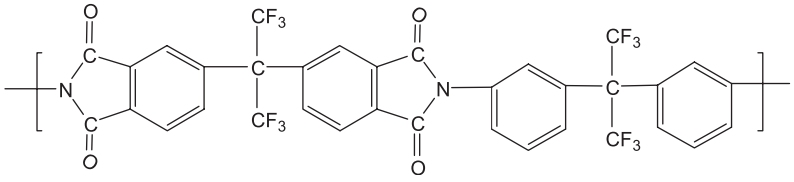

(ii) The force field used to create the above structure is replaced with a pure repulsive force field. All atoms remain in fixed locations.
(iii) A trial repulsive particle is then randomly inserted into the repulsive polymer structure and a local energy minimum is located in the repulsive force field.
(iv) After the minimum is determined, attractive interactions are turned on and the size of the test particle is adjusted until its potential interaction with all other atoms becomes zero. This size is taken as the diameter of a spherical cavity.
(v) A check is then made to determine whether the initial random inserting point is inside the cavity or not. The cavity is only accepted if the initial point is inside the cavity. This procedure leads to volume distribution rather than a number distribution of cavities.
(vi) Steps iii to v are repeated enough times to get a representative distribution of cavity sizes for a given structure.

Diffusion coefficients were determined by adding 10 neon molecules to each of 10 independent states. After each state was equilibrated for 60 ps, the diffusion constants were calculated by molecular center of mass displacement over a

Table 2
Properties of polymers used in this study [4,8,9]

Polymer	Density (g/cm^3)	FFV[a]	T_g (°C)	Measured *d*-spacing (Å)	P_{CO_2} (barrer)	P_{He} (barrer)
PSF	1.240	0.156	186	5.2	5.6	13
3,4′-PSF	1.250	0.149	156	5.3	1.5	9.3
PSF-P	1.191	0.156	191	5.4	6.8	14
PSF-M	1.201	0.151	140	5.3	2.8	11.7
6FDA-6F*p*DA	1.466	0.190	320	5.9	66	–
6FDA-6F*m*DA	1.493	0.175	254	5.7	4.4	–

T_g, glass transition temperature.
[a] FFV, fractional free volume which is obtained using the Bondi group contribution method.

Table 3
Simulation data

Polymer	Number of atoms	Density (g/cm^3)	Length of the periodic cell (Å)
PSF	542	1.24	18.12
3-4′-PSF	542	1.25	18.07
PSF-P	732	1.19	19.87
PSF-M	732	1.20	19.81
6FDA-6F*p*DA	1322	1.47	25.63
6FDA-6F*m*DA	1322	1.49	25.47

200 ps interval for PSF and 3,4′-PSF, and 120 ps interval for PSF-P, PSF-M, poly-6FDA-6F*p*DA and poly-FDA-6F*m*DA using the Einstein relationship [45]:

$$D = \lim_{t\to\infty} \frac{1}{6t} \langle [\mathbf{r}_i(t) - \mathbf{r}_i(0)]^2 \rangle \quad (1)$$

where $\mathbf{r}_i$ is the position vector of atom i, $\langle [\mathbf{r}_i(t) - \mathbf{r}_i(0)]^2 \rangle$ represents the ensemble average of the mean-square displacement (MSD) of the gas molecule trajectories; $\mathbf{r}_i(t)$ and $\mathbf{r}_i(0)$ are the final and initial position of the center of mass of the gas molecules over the time interval t. Finally, an average value of D was calculated from results of the ten independent states, and diffusion coefficient for each state was an average over 10 inserted neon molecules. Charati and Stern [22] have obtained diffusion coefficients of He, O_2, N_2, CH_4, and CO_2 in silicone polymers by inserting 4 penetrant molecules in each of five different polymer microstructures. In this work, we doubled the polymer states. The effectiveness of this 'multiple states' was proven in our recent work [36,48], where we simulated diffusion coefficients of CO_2 in PTMSP and poly[1-phenyl-2-[*p*-(trimethylsilyl)phenyl]acetylene] (PTMSDPA), and found very good agreement between simulation and experimental data.

Our simulated diffusion coefficients for CO_2 are too small compared with experimental values. Others have had difficulties with CO_2 also. Fried et al. [46], using the same COMPASS forcefield, investigated diffusion of O_2, N_2, CH_4, and CO_2 in poly(2,6-dimethyl-1,4-phenylene oxide) by means of molecular simulation. Although the simulations were run for 2 ns, agreement between simulation and experimental data was not satisfactory for CO_2. Heuchel and his co-workers [15,24] have used a different simulation technique, the Gusev–Suter transition-state theory (TST), to calculate gas diffusion coefficients for O_2, N_2, CH_4, and CO_2 in different polyimides. They observed good agreement between simulation and experimental data except CO_2. The applied TST method does not work well for CO_2 and other larger molecules. They suggested that this may be related to the anisotropic geometry of the molecule as well as stronger interactions that can induce structural relaxations, which are not considered in TST model where the dynamics of the dissolved molecules is coupled only to the elastic thermal motion of the dense polymer.

It seems that the 'big' CO_2 molecules were trapped in these relatively low-free-volume polymers, so we have studied smaller neon diffusion. The Lennard–Jones parameter, σ, of CO_2 used in united atom representation of penetrant molecules in COMPASS forcefield is 4 Å, whereas 3.13 Å for Ne, and 3.46 Å for O_2 [20]. Teplyakov and co-workers [47] have developed a correlation between diffusion coefficient D and effective penetrant diameter d_{eff} based on extensive experimental data with different gases and polymer matrices, which is:

$$\log D = K_1 - K_2 d_{\text{eff}}^2 \quad (2)$$

Where, the coefficient K_1 and K_2 depend on the chemical and physical properties of the polymer matrices. This correlation works well for both glassy and rubbery polymers, and it indicates why diffusion is so sensitive to the size of penetrant molecules. Diffusion of neon is orders of magnitude larger than CO_2. A simulation time of 120–200 ps appeared to be sufficient to obtain normal diffusive motion of neon in the isomers we studied based on the small size of neon as well the Ref. [22] and our own study [48]. Charati and Stern [22] have calculated diffusion coefficients of He, O_2, N_2, CH_4, and CO_2 in four silicone polymers from the mean square displacements (MSD) of penetrant molecules by means of the Einstein equation with a simulation time of 200 ps. Their plots of MSD vs. time are linear for all penetrant gases over a period time of about 100 ps, and all estimated diffusion coefficients, D, were determined from the linear parts of the plots. Our group [48] has simulated the diffusion coefficients of CO_2 in high free volume PTMSDPA with a simulation time of 100 ps, and measured it experimentally. Our simulation value is in very good agreement with experimental data.

There has been a concern of the influence of the system size effect in the molecular dynamics simulations of gas permeation in glassy polymers [15,28,49]. Hofmann et al. [28] have suggested that small systems could lead to artificially large diffusion coefficients due to percolating periodic 'channels'. In contrast, Neyertz and Brown [50], very recently, found that energetic and structural properties as well as solubilities, diffusivities and characterization of the void space were size independent. The question of system size dependent transport properties remains open and one that is not addressed here.

3. Results and discussion

3.1. Fractional cavity volume and average cavity size

Table 4 presents the fractional cavity volume (FCV) and the average cavity size from molecular simulations. The numerical values of diffusion of neon in the three isomer pairs are also presented along with the experimental values of CO_2 from Refs. [4,8]. The fractional cavity volume is the

Table 4
Fractional cavity volume (FCV), average cavity size $\langle x \rangle$, and diffusion coefficients of three isomer pairs

Isomer pair	Polymer	ΔT_g (K) (=*para*−*meta*)	FCV	$\langle x \rangle$ (Å)	D_{neon} 10^{-5} cm^2/s	D_{CO_2} (exp) [4,8] 10^{-8} cm^2/s
Pair 1	PSF	30	0.076	3.74	0.35±0.17	2.0
	3-4′-PSF		0.073	3.65	0.23±0.08	0.9
Pair 2	PSF-P	51	0.077	3.82	0.60±0.30	2.5
	PSF-M		0.076	3.71	0.36±0.17	1.9
Pair 3	6FDA-6F*p*DA	66	0.110	6.76	5.3±2.90	4.5
	6FDA-6F*m*DA		0.103	6.34	3.5±1.50	0.50

fraction of space occupied by spherical cavities as defined by CESA [32–35]. The average cavity size, $\langle x \rangle$, is calculated using the following equation [35]:

$$\langle x \rangle = \frac{\int_0^\infty x^3 P(v)\mathrm{d}x}{\int_0^\infty x^2 P(v)\mathrm{d}x} \quad (3)$$

where x is the cavity size and $P(v)$ is the volume distribution obtained from CESA. The FCV is around half the fractional free volume (FFV) determined by Bondi method, which indicates that not all of the free volume is in the form of well-defined spherical cavities.

Table 4 shows that all *para* isomers have larger FCV, average cavity size and diffusion coefficient than their *meta* isomers. Polyimide isomer pair (pair 3) exhibits the greatest differences and also exhibits the largest T_g difference (ΔT_g).

Cavity size distributions determined by molecular simulation for three *para* and *meta* isomer pairs are presented in Figs. 1, 3 and 5, and their cumulative distributions are presented in Figs. 2, 4 and 6. Notice that the distribution of the *para* isomers are all shifted towards larger cavity sizes relative to the *meta* isomers.

As the Figs. 1–6 indicate, the differences in the polyimide *para* and *meta* isomer are more dramatic than those in two polysulfone isomer pairs. This is consistent with the experiments [4,8]. The *para*-connected polyimide 6FDA-6F*p*DA has a ten times increase in CO_2 diffusivity, 14-fold increase in pure CO_2 permeability and a 50% lower in CO_2/CH_4 permselectivity than those of the *meta* isomer 6FDA-6F*m*DA [8]. The study of polysulfones [4] showed relatively small increases in permselectivity and small decreases in diffusion and permeation when changing the connecting bond positions form *para* to *meta*. The CO_2 permeabilities of polysulfone *para* isomers are 2–5 folds higher than those of *meta* form, and the CO_2/CH_4 permselectivities of polysulfone *para* isomers are around 10–20% lower than those of polysulfone *meta* isomers. The CO_2 diffusivities in the *para* isomers is around twice than those in the *meta* isomers.

Nevertheless, all pairs show the trend that cavity size distributions for the *para* isomers are shifted to larger values. These results are consistent with the experimental observation that at room temperature, gas diffusion in the *para* isomer is faster than in the *meta* isomer even though the *para* isomer has a higher glass transition temperature. It should be mentioned that the dynamic behavior of membrane polymers [16,33,51,52] is also important for transport properties. Analysis of the simulation results of Karayiannis et al. [16] showed that there is more segmental motion in PET (*para*) than in PEI (*meta*). What's more, the connectivity between the cavities is also important for the transport properties of membranes polymers. Our group is developing an algorithm to quantitatively describe the connectivity between the cavities [53].

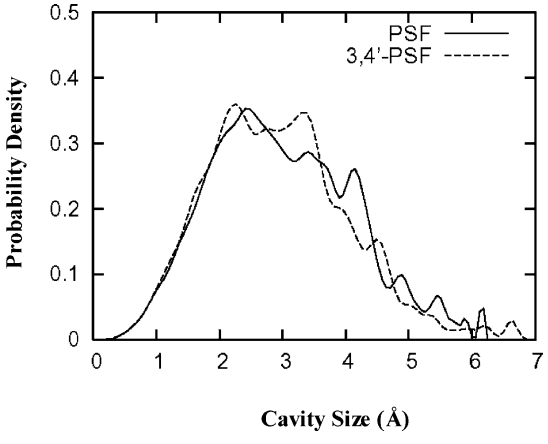

Fig. 1. Cavity size distributions in PSF(*para*) and 3,4′-PSF(*meta*) isomers at T=298 K from molecular simulation. The average cavity sizes are 3.74 Å for the *para* isomer and 3.65 Å for the *meta* isomer. The *para* isomer has higher permeability and diffusivity than the *meta* isomer (Tables 2 and 4).

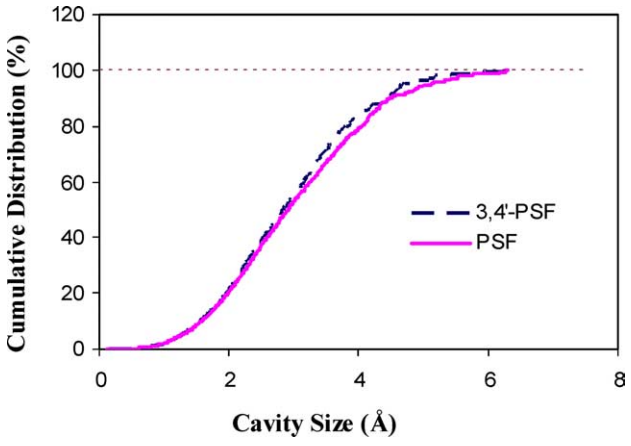

Fig. 2. Comparison of cumulative cavity size distributions in PSF (*para*) and 3,4′-PSF (*meta*).

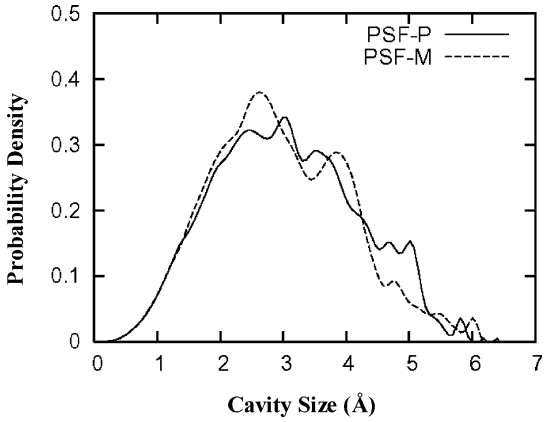

Fig. 3. Cavity size distributions in PSF-P and PSF-M isomers at $T=298$ K from molecular simulation. The average cavity sizes are 3.82 Å for the *para* isomer and 3.71 Å for the *meta* isomer. The *para* isomer has higher permeability and diffusivity than the *meta* isomer (Tables 2 and 4).

3.2. Diffusion and free volume

Diffusion coefficients of neon in these isomers were calculated using Eq. (1), and their numerical values are tabulated in Table 4. The diffusion coefficient of neon in *para* isomers is larger than in *meta* isomers, consistent with the experimental observation that gases diffuse faster in *para* isomers than in *meta* isomers. In Fig. 7, we plot the 1/FCV and 1/FFV vs. the diffusion coefficients of neon in three isomer pairs. It shows that the diffusion coefficients have an exponential relationship with FFV (or FCV), which is consistent to the free volume theory [30,31]:

$$D = A\exp\left(\frac{-B}{\mathrm{FFV}}\right) \tag{4}$$

where A and B are constants. A slight change in FFV (or FCV) will lead to a relatively dramatic change in the diffusion coefficients. Although the decrease of the FFV (or FCV) from *para* to *meta* is not very large, this small decrease yields a significant decrease in diffusivity as well as permeability (Tables 2 and 4). Takeuchi and Okazaki [54] have conducted molecular dynamics simulation of diffusion of simple gas molecules in a short chain polymer. They also found their simulated diffusion coefficients obeyed free volume theory very well.

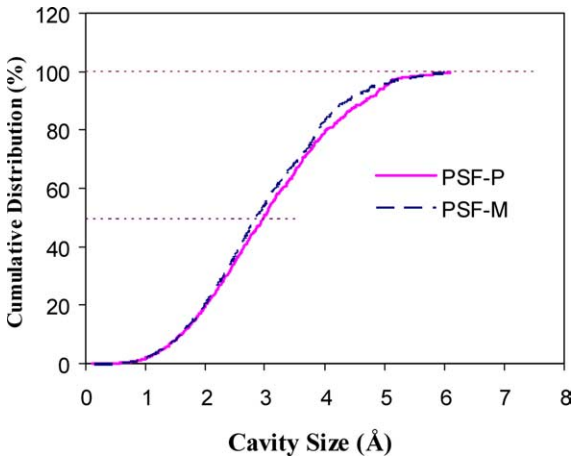

Fig. 4. Comparison of cumulative cavity size distributions in PSF-P (*para*) and PSF-M (*meta*).

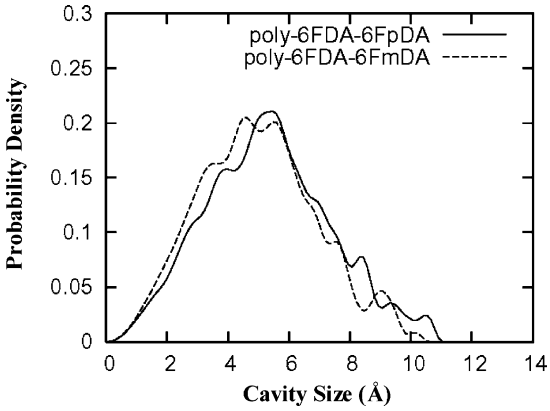

Fig. 5. Cavity size distributions in poly-6FDA-6F*p*DA and poly-6FDA-6F*m*DA isomers at $T=298$ K from molecular simulation. The average cavity sizes are 6.76 Å for the *para* isomer and 6.34 Å for the *meta* isomer. The *para* isomer has higher permeability and diffusivity than the *meta* isomer (Tables 2 and 4).

4. Conclusions

Cavity size distributions of three isomer pairs, PSF and 3,4′-PSF, PSF-P and PSF-M, 6FDA-6F*p*DA and 6FDA-6F*m*DA, have been calculated using molecular simulation. For all three isomer pairs, the cavity size distributions in the *para* isomers are shifted to larger cavities relative to the *meta* isomers. The diffusivity of neon in these isomers was also obtained by molecular dynamics. The diffusion coefficients of neon in the *para* isomers are larger than in the *meta* isomers. The larger cavities in the *para* isomers may partly contribute to their higher diffusion coefficients.

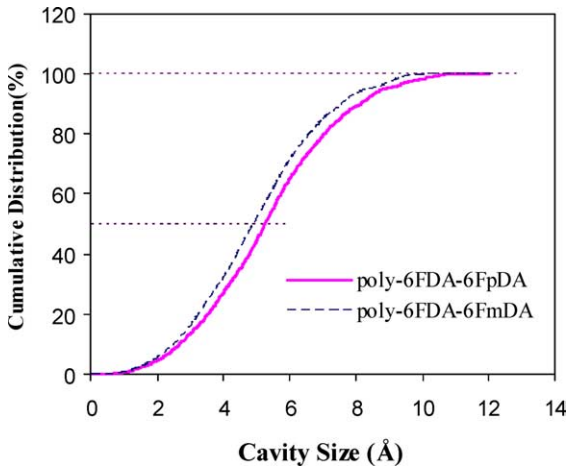

Fig. 6. Comparison of cumulative cavity size distributions in poly-6FDA-6F*p*DA (*para*) and poly-6FDA-6F*m*DA (*meta*).

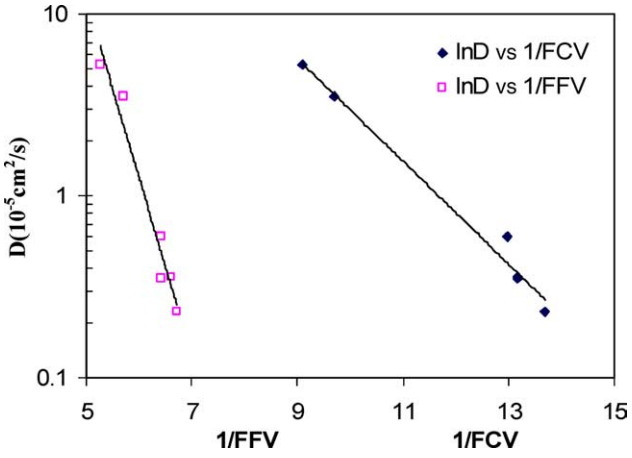

Fig. 7. Plot of ln *D* vs. 1/FFV and 1/FCV for the diffusion of neon in three pair isomers.

These results are also consistent with the experimental observation that gas diffusion in *para* isomers is faster than in *meta* isomers.

Acknowledgements

This material is based upon work supported in part by the STC Program of the National Science Foundation under Agreement No. CHE-9876674.

References

[1] Nakagawa T. In: Paul DR, Yampol'skii YP, editors. Polymeric gas separation membranes. 1st ed. Boca Raton, FL: CRC Press; 1994. p. 155.
[2] Kestinn RE, Fritzsche AK. Polymeric gas separation membranes. New York: Wiley-Interscience; 1993.
[3] Aitken CL, Koros WJ, Paul DR. Macromolecules 1992;25:3651–8.
[4] Aitken CL, Koros WJ, Paul DR. Macromolecules 1992;25:3424–34.
[5] Coleman MR, Koros WJ. J Polym Sci, Part B: Polym Phys 1994;32: 1914.
[6] Stern SA, Mi Y, Yamamoto H, St Clair AK. J Polym Sci, Part B: Polym Phys 1989;27:1887.
[7] Koros WJ, Coleman MR. Annu Rev Mater Sci 1992;22:47.
[8] Coleman MR, Koros WJ. Macromolecules 1999;32:3106–13.
[9] Coleman MR, Koros WJ. J Membr Sci 1990;50:285.
[10] Light RR, Seymour RW. Polym Eng Sci 1982;22:229.
[11] Sheu FR, Chern RT. J Polym Sci, Polym Phys Ed 1989;27:1121.
[12] Min KE, Paul DR. Polym Sci, Polym Phys Ed 1988;26:1021.
[13] Muruganandam N, Paul DR. J Membr Sci 1987;34:185.
[14] Pavel D, Shanks R. Polymer 2003;44:6713–24.
[15] Heuchel M, Hofmann D, Pullumbi P. Macromolecules 2004;37: 201–14.
[16] Karayiannis NC, Mavrantzas VG, Theodorou DN. Macromolecules 2004;37:2978–95.
[17] Tamai T, Tanaka H, Nakanishi K. Macromolecules 1994;27: 4498–508.
[18] Takeuchi H, Roe RJ, Mark JE. J Chem Phys 1990;93:9042–8.
[19] Hofmann D, Entrialgo-Castano M, Lerbret A, Heuchel M, Yampolskii Y. Macromolecules 2003;36:8528–38.
[20] Kucukpinar E, Doruker P. Polymer 2003;44:3607–20.
[21] López-González M, Saiz E, Guzman J, Riande E. J Chem Phys 2001; 115:6728–36.
[22] Charati SG, Stern SA. Macromolecules 1998;31:5529–35.
[23] Sok RM, Berendsen HJC, van Gunsteren WF. J Chem Phys 1992;96: 4699–704.
[24] Heuchel M, Hofmann D. Desalination 2002;144:67–72.
[25] Kim WK, Mattice WL. Comput Theor Polym Sci 1998;8:353–61.
[26] Hofmann D, Fritz L, Ulbrich J, Paul D. Polymer 1997;38:6145–55.
[27] Fried JR, Ren P. Comput Theor Polym Sci 2000;8:447–63.
[28] Hofmann D, Fritz L, Ulbrich J, Schepers C, Böhning M. Comput Theor Polym Sci 2000;9:293–327.
[29] Fried JR, Goyal DK. J Polym Sci, Part B: Polym Phys 1998;36: 519–36.
[30] Cohen MH, Turnbull DJ. J Chem Phys 1959;31:1164.
[31] Thran A, Kroll G, Faupel F. J Polym Sci, Part B: Polym Phys 1999;37: 3344.
[32] in 't Veld PJ, Stone MT, Truskett TM, Sanchez IC. J Phys Chem B 2000;104:12028–34.
[33] Nagel C, Schmidtke E, Günther-Schade K, Hofmann D, Fritsch D, Strunskus T, et al. Macromolecules 2000;33:2242–8.
[34] Rigby D, Roe RJ. Macromolecules 1990;23:5312–9.
[35] Wang XY, Lee KM, Lu Y, Stone MT, Sanchez IC, Freeman BD. Polymer 2004;45:3907–12.
[36] Wang XY, Lee KM, Lu Y, Stone MT, Sanchez IC, Freeman BD. Modeling transport properties in high free volume glassy polymers. In: Korugic-Karasz LS, MacKnight WJ and Martuscelli E, editors. ACS symposium series No. 916, New Polymeric Materials, in press, 2005.
[37] Schmidtke E, Günther-Schade K, Hofmann D, Faupel F. J Mol Graph Model 2004;22:309–16.
[38] Shantarovich VP, Azamatova ZK, Novikov YA, Yampolskii YP. Macromolecules 1998;31:3963–6.
[39] Shantarovich VP, Kevdina IB, Yampolskii YP, Alentiev AY. Macromolecules 2000;33:7453–66.
[40] Nagel C, Günther-Schade K, Fritsch D, Strunskus T, Faupel F. Macromolecules 2002;35:2071–7.
[41] Hofmann D, Heuchel M, Yampolskii YP, Khotimskii V, Shantarovich VP. Macromolecules 2002;35:2129–40.
[42] Singh A, Bondar S, Dixon S, Freeman BD, Hill AJ. Proc Am Chem Soc Div Polym Mater Sci Eng 1997;77:316–7.
[43] Materials Studio and Cerius2 are two packages developed by Accelrys Inc., http://www.accelrys.com/, San Diego, CA; 2002.
[44] Sun H. J Phys Chem B 1998;102:7338–64.
[45] Frenkel D, Smit B. Understanding molecular simulation. 2nd ed. London: Academic Press; 1996.
[46] Fried JR, Sadat-Akhavi M, Mark JE. J Membr Sci 1998;149:115–26.
[47] Teplyakov V, Meares P. Gas Sep Purif 1990;4:66–74.
[48] Wang XY, Raharjo RD, Lee HJ, Freeman BD, Sanchez IC. In preparation.
[49] Pinel E, Brown D, Bas C, Mercier R, Albérola ND. Macromolecules 2002;35:10198–209.
[50] Neyertz S, Brown D. Macromolecules 2004;37:10109–22.
[51] Theodorou DN. In: Neogi P, editor. Diffusion in polymers. New York: Marcel Dekker; 1996.
[52] Theodorou DN. Principles of molecular simulation of gas transport in polymers. In: Yampolskii Yu, Pinnau I, Freeman BD, editors. Materials science of membranes for gas and vapor separation. New York: Wiley; in press.
[53] Willmore FT, Sanchez IC. Recent advances in the characterization of free volume in model fluids and polymers: Shape and connectivity. NSTI Nanotech 2005.
[54] Takeuchi H, Okazaki K. J Chem Phys 1990;92:5643–52.